Combined Spin-Mass Vortex with Soliton Tail in Superfluid ^{3}He-B

Y. Kondo,[1],[a] J. S. Korhonen,[1] M. Krusius,[1] V. V. Dmitriev,[2] E. V. Thuneberg,[1] and G. E. Volovik[3]

[1]*Low Temperature Laboratory, Helsinki University of Technology, 02150 Espoo, Finland*
[2]*Kapitza Institute for Physical Problems, 117334 Moscow, U.S.S.R.*
[3]*Landau Institute for Theoretical Physics, 117334 Moscow, U.S.S.R.*

(Received 16 December 1991)

We have observed spin-mass vortices (SMV) in superfluid ^{3}He-B. The SMV is a combined topological object made up of a vortex line with mass current and a disclination line with spin current. It is also a termination line of a planar defect (θ soliton). The SMV's are bound either as pairs or to the container wall by the soliton. They are nucleated when a rotating ^{3}He sample cools slowly through the $A \rightarrow B$ phase transition. The identification of the SMV is based on the NMR signatures of the soliton.

PACS numbers: 67.50.Fi

The existence of topologically stable objects is one of the prominent consequences of broken symmetry in condensed-matter and high-energy physics. The superfluid phases of ^{3}He are the extreme example of symmetry breaking and their rich topology harbors many different types of defects [1]. Vortex lines can be stabilized by rotation, and there is experimental evidence of five different types: three in the A phase, which all belong to different topological classes, and two in the B phase, which belong to the same topological class but differ in the symmetry of their cores [2]. For other defects in ^{3}He there is no corresponding field, like rotation, which could support their equilibrium, or at least quasiequilibrium, configuration. Examples of such objects are planar defects (solitons), of which a few types may have been identified in NMR experiments.

We present the first experimental evidence of a new kind of topological object in ^{3}He-B: the combination of a vortex and a disclination. This linear object is also a termination line for a soliton, and thus an example of topological confinement of objects with different spatial dimensions. The topological stability of this hybrid of linear and planar objects is based on the same principles as that of a wall terminating on a string, or a string terminating on a monopole, which arise in some models of grand unification in particle physics [3]. Topological confinement is also observed in liquid crystals; in particular, strings terminating on point defects are reported [4]. Because of the mixed vortex and soliton properties, the triple hybrid of a vortex+disclination+soliton appears as a highly stable structure in ^{3}He-B, as depicted in Fig. 1.

Topology.—To a good approximation, the symmetry group of normal ^{3}He is $U(1)\times SO_3^{(S)}\times SO_3^{(L)}$. Here $U(1)$ is the gauge group, $SO_3^{(S)}$ the group of spin rotations, and $SO_3^{(L)}$ the group of orbital rotations. In the superfluid ^{3}He-B, this symmetry is broken in such a way that only the total rotation symmetry $SO_3^{(S+L)}$ remains [5]. Most crucial is that the B phase is degenerate with respect to both $U(1)$ and the relative rotation of spin and orbit parts. The latter will be denoted briefly by SO_3. The group $U(1)$ can be parametrized by a phase Φ (defined modulo 2π), and SO_3 by an axis $\hat{\mathbf{n}}$ and an angle θ of rotation.

The defects of the B phase can be classified simply on the grounds of the $U(1)\times SO_3$ degeneracy. There are two basically different linear objects. $U(1)$ gives rise to a conventional quantized vortex, where the phase Φ changes by 2π while encircling the line once. We call it a mass vortex (MV) because mass flow circulates around the line. Another type of linear defect corresponds to the SO_3 degeneracy. In the simplest model, the rotation angle θ changes by 2π but $\hat{\mathbf{n}}$ stays fixed while encircling the line. This object is called a disclination or a spin vortex (SV) because there is a spin current around the line. As distinct from a MV, a SV is equivalent to its antivortex since the homotopy group $\pi_1(SO_3)=Z_2$ consists of two elements 0 and 1 with the summation law $1+1=0$ [6].

We have neglected above a small spin-orbit coupling caused by the magnetic dipole-dipole interaction of ^{3}He nuclei. It lifts the SO_3 degeneracy by favoring the angle $\theta=\theta_0\approx 104°$. Because this interaction is weak, it does not affect the high-energy structure of a SV, which is characterized by the small core size $\xi\approx 0.01$ μm. It does

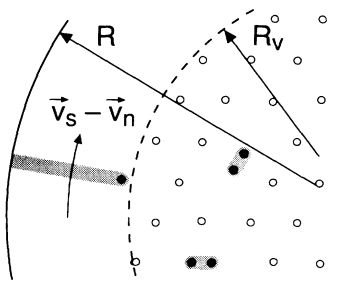

FIG. 1. Schematic cross-sectional cut of the rotating NMR cell after a slow $A \rightarrow B$ transition. Mass vortices (open dots) form a cluster separated from the cell wall by a counterflow layer. Spin vortices, which are edge lines for solitons (grey), are pinned on mass vortices to form spin-mass vortices (SMVs, black dots). SMVs appear either within the cluster as pairs bound by a soliton or on the periphery of the cluster with the soliton terminating on the cell wall.

modify, however, the low-energy, large-scale structure characterized by the dipole length $\xi_D \approx 10$ μm. Generally the fixation of a degeneracy parameter related to a line defect leads to the formation of a wall bound to the line. Here the SV becomes a termination line to a so-called θ soliton [6]. The topological structure of a SV and the associated soliton is shown in Fig. 2. On a path around the SV line, the angle θ remains equal to θ_0 outside the soliton and only $\hat{\mathbf{n}}$ changes. Within the soliton, θ increases from 104° to 180° and then decreases from 180° to 104°, but with opposite direction of $\hat{\mathbf{n}}$ [7].

Stabilization.— Because of its surface tension, a soliton tends to shrink. This makes a SV positionally unstable in the bulk, unless it is pinned. The most intriguing alternative is to pin it on a MV. Because the superfluid state is deformed within the vortex core, it is energetically more favorable for a MV and a SV to form a common core. Thus the resulting spin-mass vortex (SMV) is stable against dissociation into a SV and a MV [8]. Whenever a SV is created among MVs, it will likely be pinned by one of the MVs. This triple hybrid, spin vortex+mass vortex+soliton, may now be positionally stabilized by the balance of two forces: The surface tension σ of the soliton can be compensated by the Magnus force acting on the MV component of the hybrid. The Magnus force $F_M = \kappa\rho_s(v_s - v_n)$ arises if the superfluid velocity $v_s = \hbar\nabla\Phi/2m_3$ differs from v_n, the common velocity of the vortex and the normal fluid. Here $\kappa = \pi\hbar/m_3$ is the quantum of circulation and ρ_s the superfluid density. The stabilization is achieved in two different configurations.

A cylinder with radius R rotating with angular velocity

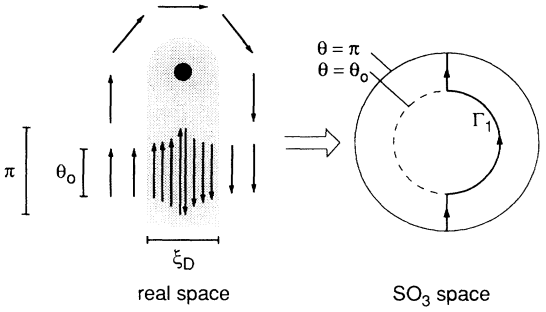

FIG. 2. Topological structure of the spin vortex (black dot) with the soliton tail (grey). The arrows indicate the vector $\hat{\mathbf{n}}\theta$ on a path encircling the SV line. On the right, the rotation group SO_3 is parametrized by the vector $\hat{\mathbf{n}}\theta$: A solid sphere of radius π has one-to-one correspondence with SO_3 when diametrically opposite points on the surface of the sphere are identified. The path around the SV is mapped to the closed contour Γ_1. The SV is topologically stable because Γ_1 cannot be continuously contracted to a point. The curved part of Γ_1 comes from the region outside the soliton where θ is fixed by spin-orbit interaction to $\theta_0 \approx 104°$. The straight parts of Γ_1 come from the region within the soliton. In contrast to this simplified figure, the lowest energy is obtained when all $\hat{\mathbf{n}}$ orientations are rotated by 90° in the plane of the paper (Fig. 4) [7].

Ω supports in equilibrium $N = \pi R^2 n$ mass vortices, where $n = 2\Omega/\kappa$ is the vortex density. It is possible to generate states with a smaller number of vortices in a controlled way in ^{3}He-B. Such states have all the vortices packed at the equilibrium density in a central cluster with radius $R_V = R(\Omega_V/\Omega)^{1/2} < R$. Here Ω_V denotes the angular velocity at which the cluster would expand to the container wall. The cluster is isolated from the wall by an annular layer which carries macroscopic counterflow of the normal and superfluid components: $v_s - v_n = \Omega_V R^2/r - \Omega r$. Consider now a SMV at a radial position r in the counterflow layer and the soliton terminating on the wall (Fig. 1). The balance $\sigma = F_M$ gives, after trivial algebra, the length of the soliton $l = R - r$:

$$\frac{l(\Omega)}{R} = 1 - \frac{\Omega_S}{2\Omega} - \left[\frac{\Omega_V}{\Omega} + \left(\frac{\Omega_S}{2\Omega}\right)^2\right]^{1/2}, \qquad (1)$$

where $\Omega_S = \sigma/\rho_s\kappa R$. Using $\sigma = 2.0 g_D \xi_D$ [7], where g_D is the dipole constant, we obtain for our cell ($R = 3.5$ mm) that $\Omega_S \approx 0.05$ rad/s is much smaller than a typical $\Omega_V \sim 1$ rad/s. Thus the SMV lies very close to the edge of the vortex cluster and the condition for the stability of the soliton is $\Omega > \Omega_V + \Omega_S \approx \Omega_V$.

In the second configuration, the soliton confines two SMVs to a pair (Fig. 1). From the outside it looks like a doubly quantized MV. The distance d of the SMVs in the pair is determined by the balance between the repulsion of the MV parts and the attraction of the SV parts. A repulsive Magnus force $F_M = \kappa^2\rho_s/2\pi d$ arises between two parallel MVs. Because a SV is equivalent to its antivortex, the force between SVs is attractive, and at large distances ($d \gg \xi_D$) it approaches the soliton tension σ. One then obtains an upper limit $d \leq \kappa^2\rho_s/2\pi\sigma$, which is about $6\xi_D$ close to T_c. This is less than the average spacing between MVs in the vortex lattice (≈ 200 μm at $\Omega = 1$ rad/s). Thus d is expected to decrease only slightly with increasing Ω when the SMV pair is placed among the other vortices in the rotating liquid.

Experiment.—Our experimental cell is a cylinder of radius $R = 3.5$ mm and height $L = 7$ mm rotating around its axis (vertical). It is connected to the rest of the ^{3}He chamber only by a small orifice in the center of the bottom plate. This suppresses the leakage of vortices from the lower part of the ^{3}He chamber to the NMR cell. The critical velocity for the nucleation of ^{3}He-B vortices in the NMR cell exceeds 2.8 rad/s at 29.3 bars and $0.6T_c < T \leq T_{AB}$. Velocities smaller than that were used in the following.

The state showing evidence of SMVs is produced as follows. The cell is continuously rotated at a velocity $\Omega_{A\to B}$. Initially, the liquid in the NMR cell is prepared to be in the A phase with an equilibrium number of A-phase vortices. The B phase is maintained in the lower part of the chamber. Then the A-B interface is gradually allowed to rise during slow cooling, until the A phase is replaced everywhere. The resulting B-phase state con-

tains less vortices than a rotating equilibrium state. The number of vortices was determined by comparing with reference states of known number of vortices [9].

More surprisingly, the state after the $A \rightarrow B$ transition clearly differs from any reference state. The difference is most prominent in a resonance mode peculiar to ^{3}He-B, which is called the homogeneously precessing domain (HPD) [10]. In this mode, both the magnetization $\mathbf{M}$ and the rotation axis $\hat{\mathbf{n}}$ precess uniformly around $\mathbf{H}$. The precession is homogeneous over the whole domain. $\mathbf{M}$ and $\hat{\mathbf{n}}$ are tilted from $\mathbf{H}$ by 104° and 90°, respectively, such that a rotation around $\hat{\mathbf{n}}$ by 104° maps $\mathbf{H}$ to $\mathbf{M}/\chi$ (χ is the static susceptibility). In contrast, a static domain (SD) has $\mathbf{M}=\chi\mathbf{H}$ and $\hat{\mathbf{n}}\|\mathbf{H}$. The HPD and SD can exist in dynamical equilibrium when a field gradient ∇H is applied. The two domains are separated by a domain wall, where $\mathbf{M}$ and $\hat{\mathbf{n}}$ change smoothly.

The usefulness of the HPD lies in the absorption due to spin diffusion, which is given by $P=\int dV D|\nabla_i \mathbf{M}|^2$. (We neglect the tensor nature of the diffusion coefficient D.) Thus the absorption is sensitive to regions where the magnetization is nonuniform, such as the HPD-SD wall, vortices, and θ solitons. In our case with a uniform $-\nabla H\|\mathbf{H}\|\boldsymbol{\Omega}$, the wall is perpendicular to the axis of the NMR cell. We monitor the total HPD absorption in a cw measurement with the domain boundary adjusted to lie just below the orifice of the NMR cell.

After the $A \rightarrow B$ transition, the HPD absorption reveals an unstable state. It exhibits large absorption which in some minutes decreases to a seemingly stable level. This level is still 10–100 times higher than the absorption due to all MVs and several times higher than the absorption due to the HPD-SD wall. This state withstands various perturbations. For example, after the state has been created at rotation velocity $\Omega_{A\rightarrow B}$, it can be studied also at different velocities Ω. Figure 3 shows the absorption $\Delta P=P_{\rm tot}-P_{\Omega=0}$ scanned as a function of Ω after three $A \rightarrow B$ transitions. Two types of behavior are observed: one is fitted well by a square-root dependence, $P(\Omega) \propto 1-(\Omega_c/\Omega)^{1/2}$ (solid lines in Fig. 3), while the other is almost constant (dashed line in Fig. 3).

Large solitons.— We associate the square-root-type absorption with a "large" soliton bound to a SMV in the counterflow layer. The main reason is that this explains the Ω dependence of the absorption: A soliton gives rise to absorption that is proportional to its area, $P(\Omega)=P(\infty)l(\Omega)/R$, where $l(\Omega)$ is given by Eq. (1). Recalling that Ω_S is small, this is what is observed. Moreover, the absorption extrapolates to zero when Ω is reduced to a critical value Ω_c. This value coincides with Ω_V at which the counterflow zone shrinks to zero, as determined independently from a measurement of the number of vortices in the cluster. The square-root absorption is irreversibly lost once Ω is reduced below Ω_V. This is readily understood because the vanishing counterflow permits the solitons to annihilate at the side walls of the NMR cell.

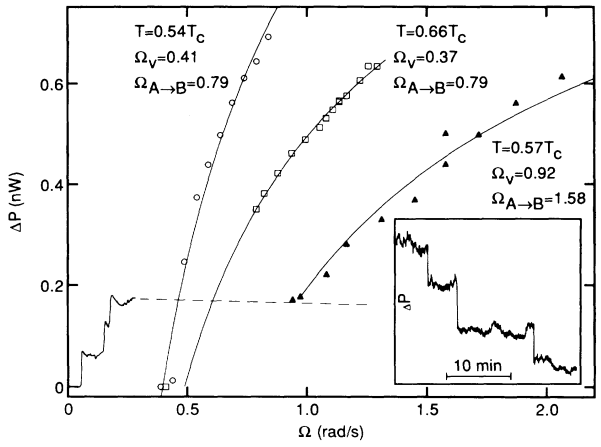

FIG. 3. HPD resonance absorption $\Delta P=P_{\rm tot}-P_{\Omega=0}$ plotted as a function of rotation speed Ω as measured after three $A \rightarrow B$ transitions. The pressure is 29.3 bars and field $H=28.4$ mT. The two examples on the left ($\Omega_{A\rightarrow B}=0.79$ rad/s) display only the square-root dependence given in Eq. (1) and are interpreted to have only solitons extending across the counterflow layer, most likely two in both cases. The curves have been fitted to the data and represent $P(\Omega)=P(\infty)[1-(\Omega_c/\Omega)^{1/2}]$. Ω_V has been determined from independent measurements of the vortex number and agrees with Ω_c, within the combined uncertainties. The third example ($\Omega_{A\rightarrow B}=1.58$ rad/s) we assign to a state with one soliton across the counterflow layer (solid curve) and three solitons inside the vortex cluster (dashed line and raw trace). Spontaneous jumps at constant $\Omega=1$ rad/s are shown in the inset. Both the square-root curves and the horizontal dashed line can be reversibly traversed up and down in Ω as long as no jumps take place.

There are other arguments in support of large solitons: (i) Simple estimate of energy gives the following picture of the HPD-soliton interaction, see Fig. 4. Instead of penetrating into the θ soliton, the HPD encloses the soliton by forming two HPD-SD walls. The wall produces absorption $\int dV D|\nabla_i \mathbf{M}|^2 \sim DM^2A/\lambda$, where A is the area and λ the thickness of the wall. For one soliton $A=2lL$. The thickness of a free HPD-SD boundary is approxi-

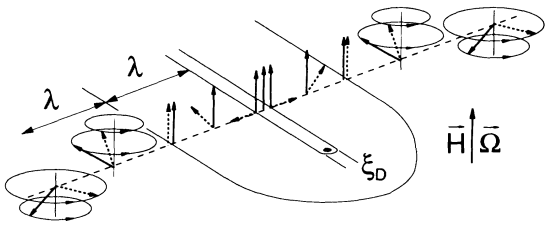

FIG. 4. Cross-sectional view of a θ soliton embedded in the HPD. Outside of the soliton, the magnetization $\mathbf{M}$ (solid arrow) and the rotation axis $\hat{\mathbf{n}}$ (dashed arrow) precess as in the bulk HPD. Inside, the soliton has a static structure with $\hat{\mathbf{n}}$ perpendicular to the soliton wall and $\mathbf{M}\|\mathbf{H}$. These two regions are separated by a HPD-SD wall. The planar soliton terminates in a SMV line (dot).

mately $\lambda_0=(c^2/\gamma^2 H\nabla H)^{1/3}$, where c is the spin-wave velocity and γ the gyromagnetic ratio [10]. The pressure of the HPD is greater inside the HPD than on its free surface. Thus at a distance $z>\lambda_0$ from the free boundary, the thickness of the boundaries covering the soliton $\lambda\approx\lambda_0^{3/2}z^{-1/2}$ is smaller than λ_0. This estimate explains the order of magnitude of the HPD absorption and also its observed $(\nabla H)^{1/2}$ dependence.

(ii) The HPD-SD boundary can be moved along the axis of the NMR cell by sweeping the magnitude of H. The distribution of the absorption is found to depend on the length h of the HPD as $h^{3/2}$, which follows from the calculation above.

(iii) The experimental absorption appears to fall in groups, which are derived with an integer multiplier from a basic one. If these units are interpreted as individual solitons, their number is usually 1–3 in the final state. The decay of the initial state is understood by the annihilation of solitons in collisions according to the summation rule $1+1=0$.

(iv) Besides the HPD mode, the ordinary NMR spectrum shows time dependence and frequency shifts expected of solitons.

(v) We do not know of any alternative explanation for our observations. The soliton bound to a SMV matches in a unique way with the observed stability and low characteristic velocity Ω_S. On the one hand, the soliton is bound topologically to the SV and the binding between the SV and MV is due to the high-energy (small-scale) structure of the vortex core. On the other hand, the position of the SMV is governed by much longer length scales associated with the vortex cluster and the dipole interaction. All other alternatives involve either a pure high-energy structure (surface states, vortices) or a pure low-energy one ($\hat{\mathbf{n}}$ or θ solitons without a SMV or metastable $\hat{\mathbf{n}}$ textures), and therefore do not show similar properties: The former cannot explain the characteristic velocities in Fig. 3 and the latter are wiped out by the HPD.

Small solitons.—The second type of the HPD absorption behavior $P(\Omega)$ is only weakly dependent on Ω (dashed line in Fig. 3). It shows up as a pedestal-like extension of the square-root curve when Ω is once reduced below Ω_V. We associate this behavior with "small" solitons bound to pairs of SMVs: (i) The size of a small soliton is almost independent of Ω, which explains the absorption $P(\Omega)$. (ii) Because of an essentially linear structure, the absorption $\int dV D|\nabla_i\mathbf{M}|^2\sim DM^2L$ is also independent of ∇H, which is consistent with measurements. (iii) Small solitons are not dependent on the presence of the counterflow layer. (iv) Downward jumps of equal magnitude, or multiples thereof, occur in the absorption level during deceleration or sometimes spontaneously (Fig. 3). These are understood as annihilations of small solitons. (v) The estimated ratios $L:A/\lambda_0:A/\lambda\approx 1:10:40$ of the absorption of a small soliton, HPD-SD boundary and large soliton $P(\infty)$ compare favorably with the experimental ones 15, 50, and 500 pW, respectively ($T=0.7T_c$, $\nabla H=5$ mT/m, and $H=14.2$ mT). As many as twenty small solitons have been counted in a vortex cluster consisting typically of 500 MVs.

In conclusion, our NMR observations match the expected properties of θ solitons. The existence of the attached SMVs is implied by the stability and velocity dependence of solitons. Thus a new class of topological objects has been found to exist as a metastable state, and the number of distinct vortices, which have been observed in ^{3}He-B, has increased from 2 to 3.

We thank O. V. Lounasmaa for discussions, Ü. Parts for help with measurements, and the Körber Stiftung and the ROTA project for support.

[a]Present address: Physics Department, University of Bayreuth, 8580 Bayreuth, Germany.

[1] N. D. Mermin, Rev. Mod. Phys. **51**, 591 (1979).
[2] P. Hakonen, O. V. Lounasmaa, and J. Simola, Physica (Amsterdam) **160B**, 1 (1989); J. P. Pekola, K. Torizuka, A. J. Manninen, J. M. Kyynäräinen, and G. E. Volovik, Phys. Rev. Lett. **65**, 3293 (1990).
[3] A. Vilenkin, Phys. Rep. **2**, 263 (1985).
[4] O. D. Lavrentovich and S. S. Rozhkov, Pis'ma Zh. Eksp. Teor. Fiz. **47**, 210 (1988) [JETP Lett. **47**, 254 (1988)].
[5] D. Vollhardt and P. Wölfle, *The Superfluid Phases of Helium 3* (Taylor & Francis, London, 1990).
[6] G. E. Volovik and V. P. Mineev, Zh. Eksp. Teor. Fiz. **72**, 2256 (1977) [Sov. Phys. JETP **45**, 1186 (1977)].
[7] K. Maki and P. Kumar, Phys. Rev. B **14**, 118 (1976).
[8] E. V. Thuneberg, Europhys. Lett. **3**, 711 (1987).
[9] Y. Kondo, J. S. Korhonen, Ü. Parts, M. Krusius, O. V. Lounasmaa, and A. D. Gongadze, Physica (Amsterdam) **178B**, 90 (1992).
[10] A. Borovik-Romanov, Yu. Bunkov, V. Dmitriev, Yu. Mukharsky, E. Poddyakova, and O. Timofeevskaya, Zh. Eksp. Teor. Fiz. **96**, 1100 (1989) [Sov. Phys. JETP **69**, 628 (1989)]; I. A. Fomin, Pis'ma Zh. Eksp. Teor. Fiz. **40**, 260 (1984) [JETP Lett. **40**, 1037 (1984)].

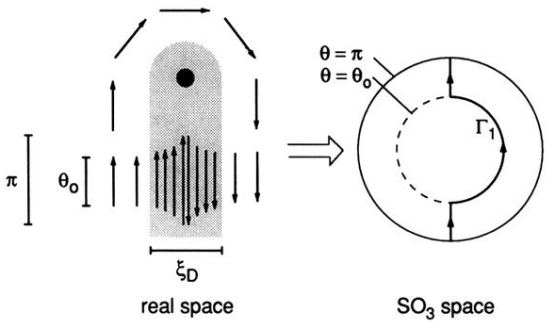

FIG. 2. Topological structure of the spin vortex (black dot) with the soliton tail (grey). The arrows indicate the vector $\hat{\mathbf{n}}\theta$ on a path encircling the SV line. On the right, the rotation group SO_3 is parametrized by the vector $\hat{\mathbf{n}}\theta$: A solid sphere of radius π has one-to-one correspondence with SO_3 when diametrically opposite points on the surface of the sphere are identified. The path around the SV is mapped to the closed contour Γ_1. The SV is topologically stable because Γ_1 cannot be continuously contracted to a point. The curved part of Γ_1 comes from the region outside the soliton where θ is fixed by spin-orbit interaction to $\theta_0 \approx 104°$. The straight parts of Γ_1 come from the region within the soliton. In contrast to this simplified figure, the lowest energy is obtained when all $\hat{\mathbf{n}}$ orientations are rotated by 90° in the plane of the paper (Fig. 4) [7].